Organo metal halide perovskites effectively photosensitize the production of singlet oxygen ($^1\Delta_g$)

Xian-Fu Zhang*[abc] and Baomin Xu*[a]

[a] Department of Materials Science and Engineering, Southern University of Science and Technology, Shenzhen, Guangdong Province 518055, China.

[b] Hebei Normal University of Science and Technology, Qinhuangdao, Hebei Province 066000, China

[c] MPC Technologies, Hamilton, Ontario, Canada L8S 3H4.

* To whom correspondence should be addressed

E-mail: xubm@sustc.edu.cn, zhangxianfu@tsinghua.org.cn. Fax: 86-755-88018904. Tel: 86-755-88018980

Abstract

Metal halide perovskite (MHP) materials are under extensive examination for various high performance optoelectronic applications, but their photosensitizing utilization for singlet oxygen generation has not been explored. Based on the observed characteristic NIR phosphorescence of singlet oxygen and the photosensitized decomposition of a specific singlet oxygen chemical trapper (diphenylisobenzofuran), we show herby that $MAPbBr_3$ quantum dots can significantly generate singlet oxygen with the quantum yield up to 0.34, which is the highest among nano semiconductor and nano metal material types of singlet oxygen photosensitizers. Further more, $MAPbBr_3$ quantum dots show good stability towards singlet oxygen. The mechanism of MHP as a singlet oxygen photosensitizer is also suggested to be due to triplet excitons. This finding expands new applications of MHPs in PDT, antiviral and antibacterial treatments, and pharmaceutical industry.

Introduction

Singlet oxygen ($^1\Delta_g$) production and its oxidizing effect are among the key interests of chemistry, biology, material and medical sciences.[1] The photosensitized singlet oxygen ($^1\Delta_g$) generation has been a fast growing research field due to its very important applications in cancer therapy,[2] antiviral and antibacterial treatments,[3] photodecomposition of organic pollutants as well as environmental protection.[3b] In addition to organic singlet oxygen photosensitizers (PSs),[4] nano semiconductors and nano metals are also proposed in recent years to act as new type of PSs,[2a, 5] but their efficiency remains low.[5a, 5c] Metal halide perovskites (MHPs) are excellent and versatile semiconductors which have shown outstanding performance in perovskite solar cells (PSCs) and light emitting diodes due to their very strong light-absorbing and light-emitting ability.[6] MHP materials are therefore under extensive studies to expand their important applications in tandem PVs,[7] water splitting architectures,[8] photodetectors,[9] and optical gain media.[10] However, their photosensitizing ability for singlet oxygen ($^1\Delta_g$) generation has not been reported in literature.

MHP materials can be good singlet oxygen photosensitizers, since they absorb light very strongly in the whole visible region[6a] which exceeds known organic PS for excited triplet state and singlet oxygen, such as porphyrin, phthalocyanine, and xanthene dyes. The MHP quantum dot (QD) is luminescent from their excited singlet exciton with quantum efficiency from 0.50 to 0.90,[6a, 6b] which gives the possible triplet exciton formation efficiency from 0.50 to 0.10. The knowledge on photosensitizing properties of MHPs is not only very valuable in finding their new

applications but also important for understanding and improving the photostability of PSCs, which is the key issue of PSC commercialization. Therefore we identify and quantify molecular singlet oxygen generated by MHP photosensitizers in this study. PSs generate singlet oxygen through following two processes: 1) light absorbing to generate its excite state *PS: PS + light $\rightarrow$ *PS; 2) energy transfer from *PS to molecular oxygen to form singlet oxygen:[11] $^{*}PS + O_2 \rightarrow PS + {}^1O_2({}^1\Delta_g)$. The *PS can be either the triplet or the singlet excited state.[12] It has been theoretically predicted that $MAPbX_3$ (X= Br, I) type perovskites can form excited triplet excitons due to spin-orbital interaction.[13] Taking all this into consideration together, we decide to test the ability of $MAPbX_3$ ($MA=CH_3NH_3$, X=Br, I) nano particles (NPs) in photosensitizing generation of singlet oxygen ($^1\Delta_g$). Using the characteristic NIR phosphorescence of singlet oxygen and the specific singlet oxygen chemical trapping agent, we show herby that $MAPbBr_3$ QD can significantly generate singlet oxygen with the quantum yield up to 0.34, which is the highest among nano-particle (metal and semiconductor nano materials) singlet oxygen photosensitizers.

Results and Discussion

(1) Perovskite NPs preparation and characterization

$MAPbBr_3$ QDs are prepared facilely by mixing MABr and $PbBr_2$ in air saturated solvent. $MAPbI_3$ QDs, however, need to be synthesized in the inert gas atmosphere. $MAPbBr_3$ QDs are also stable in air saturated solvent longer than three months, while $MAPbBr_xI_{3-x}$ (x=0,1) QDs are quickly faded upon exposing to air. We therefore focus

on $MAPbBr_3$ QDs in this study. Figure 1 shows the XRD and TEM of $MAPbBr_3$ QDs. X-ray powder diffraction peaks match the reported XRD patterns of $MAPbBr_3$ crystal,[14] indicating that a single-phase $MAPbBr_3$ was formed and thus used in the subsequent optical measurements. TEM image (Figure 1) shows that the $MAPbBr_3$ particles are spherical with median size of 5.5 nm. The UV-Vis absorption spectrum shows a band edge at ≈2.41 eV (514 nm), which is close to the onset of the band edge at 2.40 eV in literature.[15] Figure 1 also displays the photoluminescence spectrum, the emission peak maximum is at 2.40 eV (≈517 nm) in toluene with an approximate Stokes shift of 14 meV, the photoluminescence quantum yield is 0.64 which comparable to that reported (0.50 to 0.70).[15]

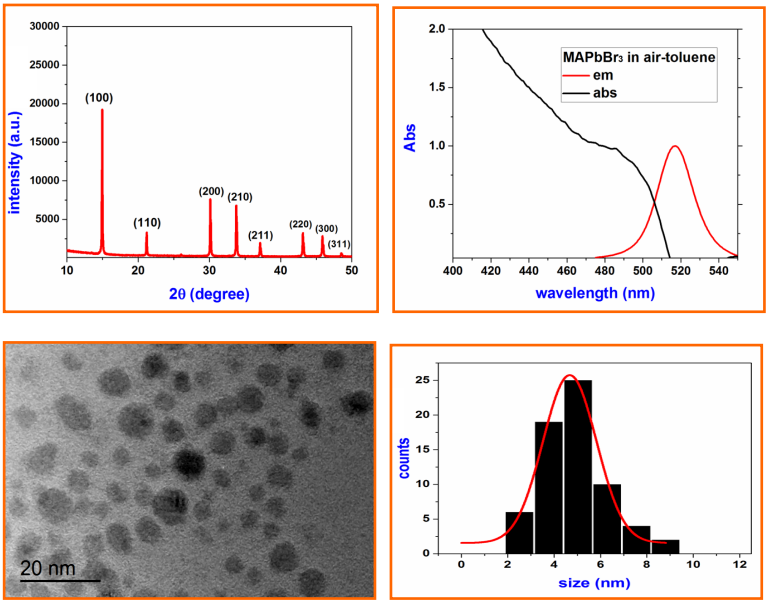

Figure 1. Top left: the XRD of $MAPbBr_3$ nano particles. **Top right**: The absorption and emission spectra of $MAPbBr_3$ NPs in toluene (excitation wavelength is 440 nm for em. spectrum).

(2) Detection of singlet oxygen by NIR photoluminescence .

The first evidence for singlet oxygen produced by the nanoscaled perovskite

photosensitization is the observed characteristic NIR emission band (Figure 2). The NIR photoluminescence shows the peak maximum at 1272±2 nm in toluene, chloroform and carbon tetrachloride. The band position and band shape very well matches that of singlet oxygen ($^1\Delta_g$) in literature.[11] In the absence of perovskite NPs control experiments show that the photoexcitation did not result in any detectable singlet oxygen emission signal. The NIR emission lifetime is 23 μs in toluene and 170 μs in chloroform. The lifetime values are also consistent with that of singlet oxygen ($^1\Delta_g$) in literature.[16] I_2-TMBDP is a well known singlet oxygen photosensitizer, its NIR emission spectra and emission decay were also measured and shown in Figure 2 for comparison. Both the emission spectrum and lifetime of I_2-TMBDP sensitized singlet oxygen is consistent with that for $MAPbBr_3$ NPs.

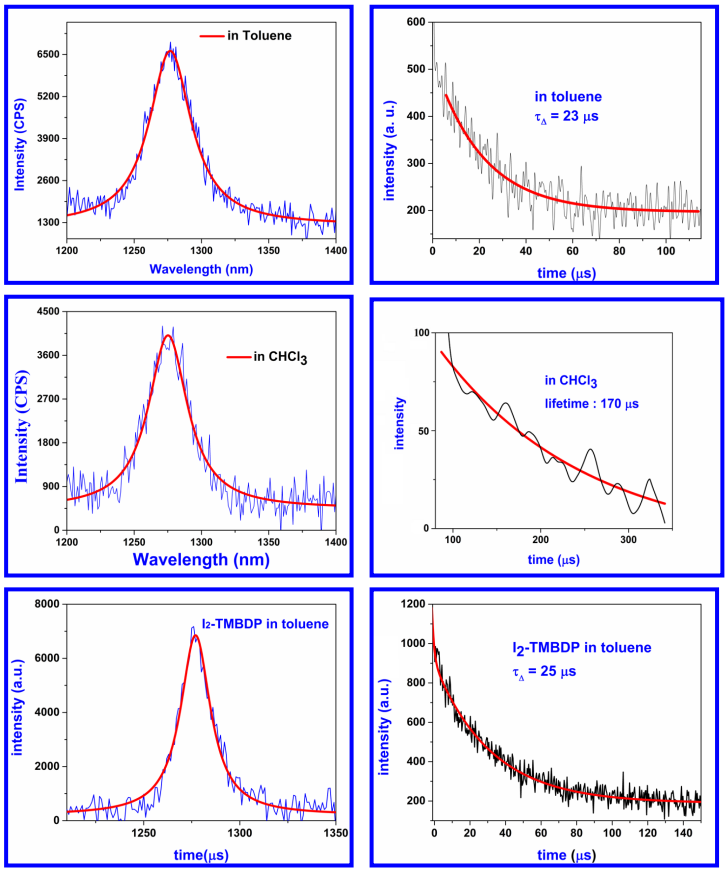

Figure 2. The NIR emission spectrum and emission decay of $MAPbBr_3$ NPs in toluene (Top) and

chloroform (Middle). The bottom is the NIR emission spectrum and emission decay of I_2-TMBDP in toluene. Excitation wavelength is 440 nm (the absorbance at this wavelength is 0.30).

(3) Detection of singlet oxygen by chemical trapping and Φ_Δ

DPBF is a well known specific chemical trapper of singlet oxygen.[17] One singlet oxygen molecule reacts very quickly with one DPBF molecule and leads to the decomposition of DPBF π system which causes the decrease of UV-Vis absorption band at 410 nm of DPBF. Figure 3 shows the change of DPBF absorption spectra in toluene containing the perovskite NPs upon light irradiation at 473 nm.

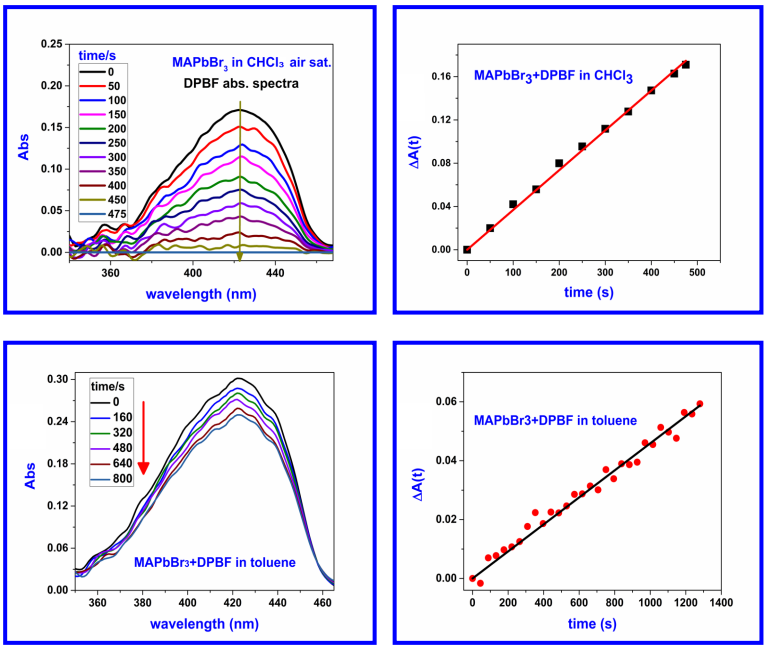

Figure 3. (Top Left) the change of DPBF (10 μM) absorption spectra in chloroform after subtracting the absorption spectrum of perovskite NPs. **(Top Right)** the plotting of A(0)-A(t) at 420 nm against time t for the measurement in $CHCl_3$, A(t) is the absorbance at time t at 420 nm. **(Bottom Left)** the change of DPBF (15 μM) absorption spectra in toluene after subtracting the absorption spectrum of perovskite NPs. **(Bottom Right)** the plotting of A(0)-A(t) at 420 nm against time t for the measurement in toluene. Pure DPBF absorption decrease is obtained by subtracting the constant absorption of the perovskites NPs.

The photo irradiation was carried out at 473 nm in air saturated solvents. At the

wavelength of 473 nm, the light is absorbed by perovskite NPs but not by the DPBF based on their individual absorption spectrum. Figure 3 clearly shows that the DPBF absorption is decreased while the absorption of perovskite NPs is not changed with time during photo irradiation. Control experiments showed that the DPBF absorption was not decreased under following conditions: 1) oxygen is purged by argon bubbling, 2) the perovskites NPs is not added to the solution, or 3) light irradiation is not carried out. These experiments clearly indicate that the DPBF decomposition needs the coexistence of perovskites NPs, oxygen, and light irradiation. These facts show that the perovskite NPs act as the singlet oxygen photosensitizer.

The chemical kinetics of DPBF decomposition is zero order as shown in Figure 3, since the plotting of A_0-A_t against time t is linear (at 420 nm): A_0-A_t = k • t, in which k is the reaction rate constant, A_0 and A_t is the absorbance of 420 nm at irradiation time zero and time t, respectively. From the linear plotting (Figure 3), the reaction rate constant k is obtained for the perovskite NP photosensitizer in each solvent. In the same way, the reaction rate constant k^{ref} is obtained for the standard photosensitizer in the same solvent. Comparing k and k^{ref}, we can obtain the singlet oxygen formation quantum yield Φ_Δ using $\Phi_\Delta=\Phi_\Delta^{ref}\cdot(k/k^{ref})\cdot(I_a^{ref}/I_a)$. The calculated Φ_Δ for the perovskite NP photosensitizer changes batch to batch samples, it is 0.34 to 0.21 in chloroform and 0.21 to 0.11 in toluene. The highest Φ_Δ value of 0.34 makes it an effective singlet oxygen photosensitizer. In fact this Φ_Δ value of 0.34 exceeds that for semiconductor and metal NP photosensitizers.[5a] For example, Φ_Δ value for Ag, Pt, and Au nano particle PSs is 0.155, 0.085, and 0.037 respectively,[5a] while Φ_Δ value of

CdSe QDs is only ~5%,[18] all of which are significantly smaller than that of the $MAPbBr_3$ NPs.

(4) Mechanism of singlet oxygen formation: singlet or triplet excitons?

The NIR emission and DPBF chemical trapping studies show that the nanoscaled perovskites are the singlet oxygen photosensitizer (PS), together with the controlled experiments, we conclude that DPBF is decomposed through the following processes in which *PS is an exciton of the perovskites NPs.

i) PS + light → *PS,

ii) *PS + O_2 → PS + $^1O_2(^1\Delta_g)$,

iii) DPBF + $^1O_2(^1\Delta_g)$ → decomposed DPBF.

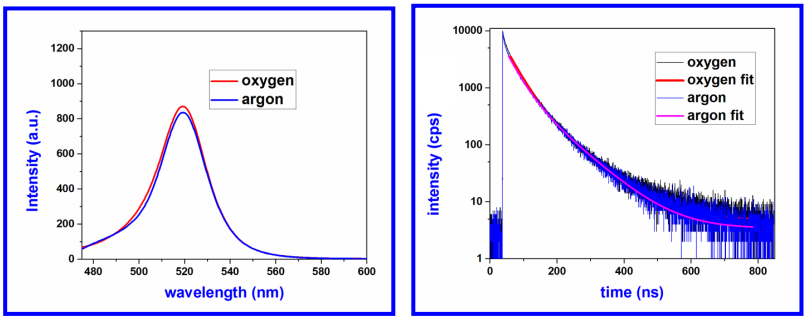

Figure 4. Left: Emission spectra of $MAPbBr_3$ NPs in argon- and oxygen-saturated toluene with excitation at 440 nm. **Right**: 520 nm emission decay of $MAPbBr_3$ NPs in argon- and oxygen-saturated toluene with excitation at 405 nm.

For organic photosensitizers, the *PS is often an excited triplet state molecule ^{3}PS, but it can also be an excited singlet state ^{1}PS in some cases.[12] Is it a singlet exciton in our case? Figure 4 shows the photoluminescence of the NPs in argon and oxygen

saturated solvent respectively. Since oxygen shows little quenching to the emission intensity and lifetime of $MAPbBr_3$ NP singlet exitons (Figure 4), indicateing that the singlet excitons do not interact with molecular oxygen remarkably. Therefore the contribution from singlet exciton of the NPs to the singlet oxygen generation is negligible. The triplet excitons are concluded to play essential roles in the singlet oxygen formation process. This conclusion is also supported by (**1**) the theoretical calculation by Li who have shown that triplet excitons of perovskites are formed by spin-orbit interactions between Pb and halogen atoms in lead halide perovskites;[13] and (**2**) the triplet exciton presence is evidenced by the phosphorescence reported by Younts.[19]

(5) Stability of $MAPbBr_3$ NPs towards singlet oxygen

It is important to know that if $MAPbBr_3$ NPs are stable to singlet oxygen. Therefore we measured the stability of $MAPbBr_3$ NPs toward singlet oxygen generated by using a very efficient photosensitizer I_2-TMBDP. As shown in Figure 5, the absorbance of $MAPbBr_3$ NPs (330, 430, and 470 nm) shows no change upon light irradiation at 540 nm in toluene. In comparison, DPBF absorbance is decreased quickly under the condition. This fact shows that $MAPbBr_3$ NPs are fairly stable to singlet oxygen.

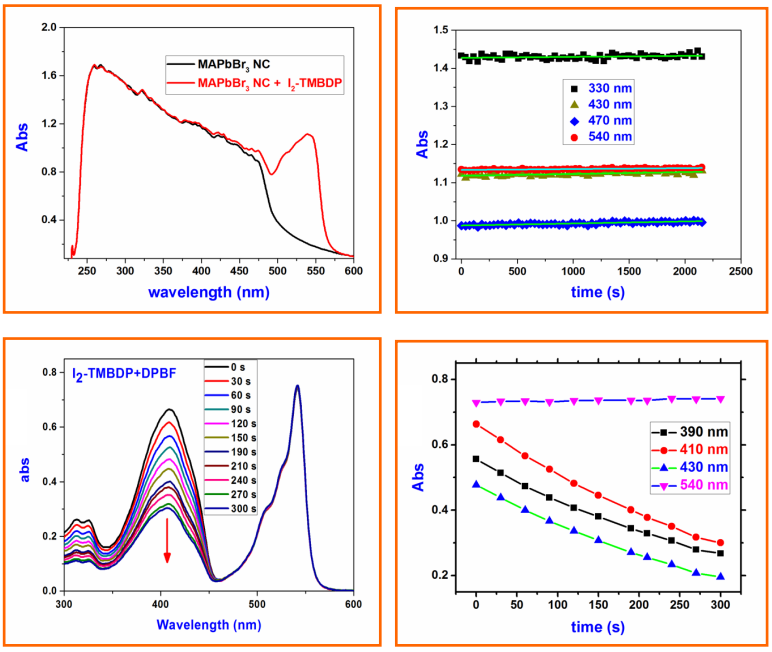

Figure 5. Top figures show that $MAPbBr_3$ NCs are stable to singlet oxygen generated by the I_2-TMBDP photosensitizer (10 μM) with photo excitation at 540 nm in toluene. **Top left:** the absorption spectra of $MAPbBr_3$ NCs in the presence and absence of I_2-TMBDP; **Top right:** the absorbance change of $MAPbBr_3$ NCs (330, 430, 470 nm) in toluene with 540 nm light irradiation time. **Bottom** figures show that DPBF decomposed quickly by singlet oxygen generated by the I_2-TMBDP photosensitizer (10 μM) with photo excitation at 540 nm in toluene. **Bottom left:** the decrease of absorption spectra of DPBF in the presence of I_2-TMBDP; **Bottom right:** the absorbance change of DPBF (390, 410, 430 nm) in toluene with 540 nm light irradiation time.

Conclusions

We have detected and quantified singlet oxygen formation photosensitized by perovskites for the first time. $MAPbBr_3$ NPs have the quantum yield up to 0.34 which is the highest among semiconductor and metal nano materials photosensitizers. $MAPbBr_3$ NPs are also fairly stable to singlet oxygen. It is the triplet exciton of $MAPBBr_3$ NPs that is mainly responsible for singlet oxygen generation. This finding suggests new potential applications of perovskite NPs in PDT, antiviral and

antibacterial treatments, and pharmaceutical industry.

Experimental Section

Materials. Methyl ammonium bromide (CH_3NH_3Br = MABr, 99.9%), lead (II) bromide ($PbBr_2$, 99.99% trace metals basis), N,N-dimethylformamide (DMF, anhydrous, 99.8%), toluene anhydrous (99.5%), chloroform anhydrous (99.5%), diphenylisobenzofuran (DPBF, 99.5%) were purchased from Sigma-Aldrich. Chloroform (>99%) and toluene (>99%). Octylamine (approximate C_{18}-content 80-90%) was purchased from Acros Organics. Oleic acid (97%) was purchased from VWR Chemicals.

Instruments. The UV-Vis electronic absorption spectra were obtained by using either Lambda 950 of Perkin-Elmer or Black CXR-SR-50 of StellnarNet Inc. Time resolved NIR and Vis photoluminescence were recorded by Fluorolog-3 fluorescence spectrometer of Horiba Scientific. Steady state Vis photoluminescence was measured by FLS920 fluorescence spectrometer of Edinburgh Instruments.

Perovskites nano particles (NPs) preparation. The synthesis were carried out according to reported method for $CH_3NH_3PbX_3$ (X=I, Br) with slight modification.[15] All syntheses were carried out at room temperature in air with average room humidity ~60%.

$MAPbBr_3$ NPs. CH_3NH_3Br (0.0088 g, 0.1 mmol) and $PbBr_2$ (0.0367 g, 0.1 mmol) were dissolved in 2.5 mL DMF containing 250 µL of the oleic acid and 10 µL octylamine. Next, 50 µL of this mixture was injected into 5 mL of toluene or

chloroform. Bright green light-emitting NPs were formed immediately after fast agitation. After centrifugation at 8000 rpm for 5 min, the clear liquid part was used for various measurements.

Methods

Perovskites NC characterization.

TEM. TEM and HRTEM images were obtained from a TEM Tecnai F30 (FEI company) high-resolution transmission electron microscope (300 kV acceleration voltage, 0.20 nm point resolution, and 0.102 line resolution), equipped with a LaB6 filament and a CCD camera with an image size of 2048×2048 pixels. TEM samples were prepared by casting one drop of the perovskites NPs in toluene onto a standard copper grid coated with a continuous amorphous carbon film, it is washed twice by n-hexane to remove oleic acid and then dried in vacum. The size distribution and thicknesses of NPs were obtained from the TEM image with ImageJ software.

X-ray Powder Diffraction (XRD). X-ray powder diffraction was obtained by the classical ex situ Bragg–Brentano geometry using a Rigaku Smartlab powder diffractometer with filtered Cu-Kα radiation and equipped with scintillation detector and two-dimensional silicon array detector. Sample preparation is as following. The concentrated toluene NP solution was centrifuged to get solid NPs, and the obtained solid NPs were washed twice by dispersing in n-hexane and centrifuged to get solid NPs again. The dried powder was used for XRD measurements.

Photophysics. The absorption and photoluminescence spectra, photoluminescence quantum yields and photoluminescence lifetimes were investigated at room temperature ca 21 ºC.

Steady-state photoluminescence spectra and quantum yields were acquired on a FLS920 of Edinburgh Instruments, the excitation wavelength of 470 nm was employed for both fluorescein and perovskites NPs. All spectra were corrected for the sensitivity of the photo-multiplier tube. The photoluminescence quantum yield (Φ_f) was calculated by using Eq. (1),[20]

$$\Phi_f = \Phi_f^0 \cdot \frac{F_s}{F_0} \cdot \frac{A_0}{A_s} \frac{n_s^2}{n_0^2}, \qquad \text{Eq. (1)}$$

in which **F** is the integrated fluorescence intensity, **A** is the absorbance at excitation wavelength, n is the refractive index of the solvent used, the subscript 0 stands for a reference compound and s represents samples. Fluorescein was used as the reference (Φ_f^0 = 0.92 in 0.1 M NaOH aq. solution).[20b] The sample and reference solutions were prepared with the same absorbance (A_i) at the excitation wavelength (near 0.09 per cm).

Photoluminescence lifetime was measured by time-correlated single photon counting method (Horiba Scientific, Fluorolog-3 spectrophotometer) with excitation at 485 nm diode laser (50 ps FWHM) and emission was monitored at 510 nm. The lifetime values were fit by biexponential decay function $I(t)=A+B_1\exp(-t/\tau_1) +B_2\exp(-t/\tau_2)$.

Singlet oxygen NIR phosphorescence. The NIR steady state photoluminescence spectra were recorded by Fluorolog-3 spectrophotometer equipped with an electronic

cooled InGaAs detector (900-1700 nm) with excitation at 400 nm using a standard 1 cm quartz cuvettes. Both the emission and excitation slits were adjusted to their maxima. A long pass filter of 1000 nm was placed between a sample and the detector for all NIR experiments to filter away any stray light and the second harmonic of the excitation light with wavelengths shorter than 1000 nm. For singlet oxygen lifetime measurements, the excitation source is changed to a 1 μs flash lamp (450 nm, 1 mW), the emission at 1270 nm was monitored.

Singlet oxygen chemical trapping. Singlet oxygen quantum yield (Φ_Δ) were determined using the well known chemical trapping method.[21] Typically, a 3 mL toluene that contains perovskites NPs and 20 μM diphenylisobenzofuran (DPBF) was irradiated at 473 nm by a LED light under air (or oxygen) saturated condition. Φ_Δ value was obtained by the relative method using Eq. (2):

$$\Phi_\Delta = \Phi_\Delta^{ref} \frac{k}{k^{ref}} \frac{I_a^{ref}}{I_a}, \qquad \text{Eq. (2)}$$

where Φ_Δ^{ref} is the singlet oxygen quantum yield for the reference standard I_2-TMBDP (2,6-diiodotetramehylBODIPY, Φ_Δ^R=0.96 in toluene) with excitation at 473 nm),[22] k and k^{ref} are the DPBF photo-bleaching rate constants in the presence of the respective sample and the reference standard, respectively; I_a and I_a^{ref} are the rates of light absorption at the irradiation wavelength of 473 nm by the samples and the reference standard, respectively. Their ratio can be obtained by Eq. (3).

$$\frac{I_a^{ref}}{I_a} = \frac{1-10^{-A_{ref}}}{1-10^{-A}}, \qquad \text{Eq. (3)}$$

In which, A and A_{ref} is the absorbance of a sample and the reference compound at

excitation wavelength 473 nm, respectively. DPBF degradation was monitored by UV-vis absorption spectrum. The error in the determination of Φ_Δ was ~10% (determined from several Φ_Δ values).

Acknowledgements

We thank the financial support from the National Key Research and Development Project funding from the Ministry of Science and Technology of China (Grants Nos. 2016YFA0202400 and 2016YFA0202404), the Peacock Team Project funding from Shenzhen Science and Technology Innovation Committee (Grant No. KQTD2015033110182370), and Hebei Provincial Hundred Talents Plan (Contract E2013100005).

Key words: Metal halide perovskites; singlet oxygen; PDT; photosensitizer.

References

[1] a) A. A. Ghogare, A. Greer, *Chem. Rev.* **2016**, *116*, 9994-10034; b) J. Park, D. Feng, S. Yuan, H. C. Zhou, *Angew. Chem. Int. Ed.* **2015**, *54*, 430-435; c) W. Fudickar, T. Linker, *Angew. Chem. Int. Ed.* **2018**, *57*, 12971-12975; d) N. Mahne, S. E. Renfrew, B. D. McCloskey, S. A. Freunberger, *Angew. Chem. Int. Ed.* **2018**, *57*, 5529-5533; e) Z. Zhou, J. Song, R. Tian, Z. Yang, G. Yu, L. Lin, G. Zhang, W. Fan, F. Zhang, G. Niu, L. Nie, X. Chen, *Angew. Chem. Int. Ed.* **2017**, *56*, 6492-6496; f) R. Toftegaard, J. Arnbjerg, K. Daasbjerg, P. R. Ogilby, A. Dmitriev, D. S. Sutherland, L. Poulsen, *Angew. Chem. Int. Ed.* **2008**, *47*, 6025-6027.

[2] a) H. Abrahamse, M. R. Hamblin, *Biochem. J.* **2016**, *473*, 347-364; b) N. Mehraban, H. S. Freeman, *Materials* **2015**, *8*, 4421-4456.

[3] a) L. Fernández, Z. Lin, R. J. Schneider, V. I. Esteves, Â. Cunha, J. P. C. Tomé, *ChemPhotoChem* **2018**, *2*, 596-605; b) D. García-Fresnadillo, *ChemPhotoChem* **2018**, *2*, 512-534.

[4] a) J. Schmitt, V. Heitz, A. Sour, F. Bolze, H. Ftouni, J.-F. Nicoud, L. Flamigni, B. Ventura, *Angew. Chem. Int. Ed.* **2015**, *54*, 169-173; b) X. Ding, B.-H. Han, *Angew. Chem. Int. Ed.* **2015**,

54, 6536-6539.

[5] a) R. Vankayala, A. Sagadevan, P. Vijayaraghavan, C.-L. Kuo, K. C. Hwang, *Angew. Chem. Int. Ed.* **2011**, *50*, 10640-10644; b) S. Wang, R. Gao, F. Zhou, M. Selke, *J. Mater. Chem.* **2004**, *14*, 487-493; c) S. S. Lucky, K. C. Soo, Y. Zhang, *Chem. Rev.* **2015**, *115*, 1990-2042; d) Y. Ma, X. Li, A. Li, P. Yang, C. Zhang, B. Tang, *Angew. Chem. Int. Ed.* **2017**, *56*, 13752-13756; e) Y. M. Sawada, Y. Nosaka, V. Biju, *Angew. Chem. Int. Ed.* **2013**, *52*, 10559-10563.

[6] a) J. S. Manser, J. A. Christians, P. V. Kamat, *Chem. Rev.* **2016**, *116*, 12956-13008; b) Q. Shan, J. Song, Y. Zou, J. Li, L. Xu, J. Xue, Y. Dong, B. Han, J. Chen, H. Zeng, *Small* **2017**, *13*, 1701770; c) S. D. Stranks, H. J. Snaith, *Nat. Nanotech.* **2015**, *10*, 391-402; d) M. Saliba, J.-P. Correa-Baena, M. Grätzel, A. Hagfeldt, A. Abate, *Angew. Chem. Int. Ed.* **2018**, *57*, 2554-2569.

[7] D. Zhao, C. Chen, C. Wang, M. M. Junda, Z. Song, C. R. Grice, Y. Yu, C. Li, B. Subedi, N. J. Podraza, X. Zhao, G. Fang, R.-G. Xiong, K. Zhu, Y. Yan, *Nat. Energy* **2018**, *3*, 1093-1100.

[8] a) V. Andrei, R. L. Z. Hoye, M. Crespo-Quesada, M. Bajada, S. Ahmad, M. D. Volder, R. Friend, E. Reisner, *Adv. Energy Mater.* **2018**, *8*, 1801403; b) G. Volonakis, F. Giustino, *Appl. Phys. Lett.* **2018**, *112*, 243901.

[9] S.-F. Leung, K.-T. Ho, P.-K. Kung, V. K. S. Hsiao, H. N. Alshareef, Z. L. Wang, J.-H. He, *Adv. Mater.* **2018**, *30*, 1704611.

[10] a) M. Li, Q. Wei, S. K. Muduli, N. Yantara, Q. Xu, N. Mathews, S. G. Mhaisalkar, G. Xing, T. C. Sum, *Adv. Mater.* **2018**, *30*, 1707235; b) N. K. Pathak, P. S. Kumar, R. P. Sharma, *Plasmonics* **2018**, *https://doi.org/10.1007/s11468-018-0778-3*, 1-8.

[11] M. C. DeRosa, R. J. Crutchley, *Coord. Chem. Rev.* **2002**, *233-234*, 351-371.

[12] C. Schweitzer, R. Schmidt, *Chem. Rev.* **2003**, *103*, 1685-1757.

[13] W. Li, L. Zhou, O. V. Prezhdo, A. V. Akimov, *ACS Energy Lett.* **2018**, *3*, 2159-2166.

[14] M. A. Najeeb, Z. Ahmad, R. A. Shakoor, A. Alashraf, J. Bhadra, N. J. Al-Thani, S. A. Al-Muhtaseb, A. M. A. Mohamed, *Opt. Mater.* **2017**, *73*, 50-55.

[15] F. Zhang, H. Zhong, C. Chen, X.-g. Wu, X. Hu, H. Huang, J. Han, B. Zou, Y. Dong, *ACS Nano* **2015**, *9*, 4533-4542.

[16] E. Boix-Garriga, B. Rodríguez-Amigo, O. Planas, S. Nonell, in *Singlet Oxygen Applications in Biosciences and Nanosciences Vol. 1* (Eds.: S. Nonell, C. Flors), Royal Society of Chemistry, Cambridge, **2016**, p. 31.

[17] P. B. Merkel, D. R. Kearns, *J. Am. Chem. Soc.* **1972**, *94*, 7244.

[18] A. C. S. Samia, X. B. Chen, C. Burda, *J. Am. Chem. Soc.* **2003**, *125*, 15736-15737.

[19] R. Younts, H.-S. Duan, B. Gautam, B. Saparov, J. Liu, C. Mongin, F. N. Castellano, D. B. Mitzi, K. Gundogdu, *Adv. Mater.* **2017**, *29*, 1604278.

[20] a) X.-F. Zhang, Y. Zhang, L. Liu, *Journal of Luminescence* **2014**, *145*, 448-453; b) X.-F. Zhang, J. Zhang, L. Liu, *J. Fluoresc.* **2014**, *24*, 819-826.

[21] F. Wilkinson, W. P. Helman, A. B. Ross, *J. Phys. Chem. Ref. Data* **1993**, *22*, 113-262.

[22] X.-F. Zhang, *J. Photochem. Photobiol. A: Chemistry* **2018**, *355*, 431-443.